

# Intro to Fusion & Intro to Tokamaks

八年李白玩家 Jacob 老师

# Intro to Fusion

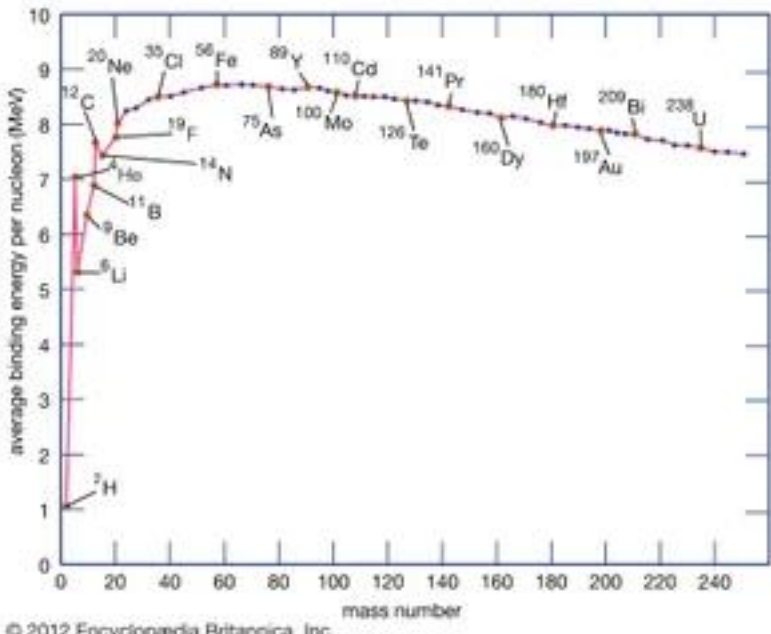
现在是——科普时间！

# Intro to Fusion 参考文献

- Oxford Physics Short Option S16
- Miscellaneous 来自网络的图片

# 一些概念

- Binding energy, Lawson criteria, 与燃料选择



## 8.2. THE LAWSON CRITERION

117

### 8.2 The Lawson Criterion

In order to achieve energy gain the reacting nuclei must be confined long enough for a sufficient number of them to fuse together. The fusion energy released per unit volume,  $E_f$ , in a D-T reaction can be written as

$$E_f = n_D n_T \sigma W \tau , \quad (8.3)$$

where  $n$  is the number density of the ions,  $\sigma$  the Maxwellian-averaged reaction rate,  $W$  the energy released per reaction, and  $\tau$  the confinement time. Assuming an equal number of Deuterium and Tritium ions,  $n_D = n_T = n/2$ ,

$$E_f = \frac{n^2 \sigma W \tau}{4} . \quad (8.4)$$

The energy required,  $E_t$  to heat the fuel to thermonuclear temperature, is given by

$$E_t = \frac{3}{2} n k_B T_i + \frac{3}{2} n_e k_B T_e = 3 n k_B T , \quad (8.5)$$

where we have assumed  $T_e = T_i$  for convenience.

In order to get energy gain, we need to get more energy out from the fusion reaction than we put in to heat up the plasma, i.e. we require  $E_f > E_t$ :

$$n \tau > \frac{12 k_B T}{\sigma W} . \quad (8.6)$$

This condition is known as the Lawson criterion. As we would expect, the density-confinement time product is a constant. A low density plasma needs to be confined for a long time in order for enough fusion reactions to occur in order for the fusion energy out to exceed the energy we put in to heat up the plasma in the first place. The denser the plasma, the shorter the necessary confinement time. Given the reaction rate shown in Fig. 8.1, which has a value of approximately  $10^{-22} \text{ m}^3/\text{s}$  at a temperature of 10 keV, and that the energy produced per reaction is 17.6 MeV, we find that we require  $n \tau > 10^{20} \text{ s m}^{-3}$ .

注意这里的 $v\sigma$ 就是中间图里的 $\sigma$

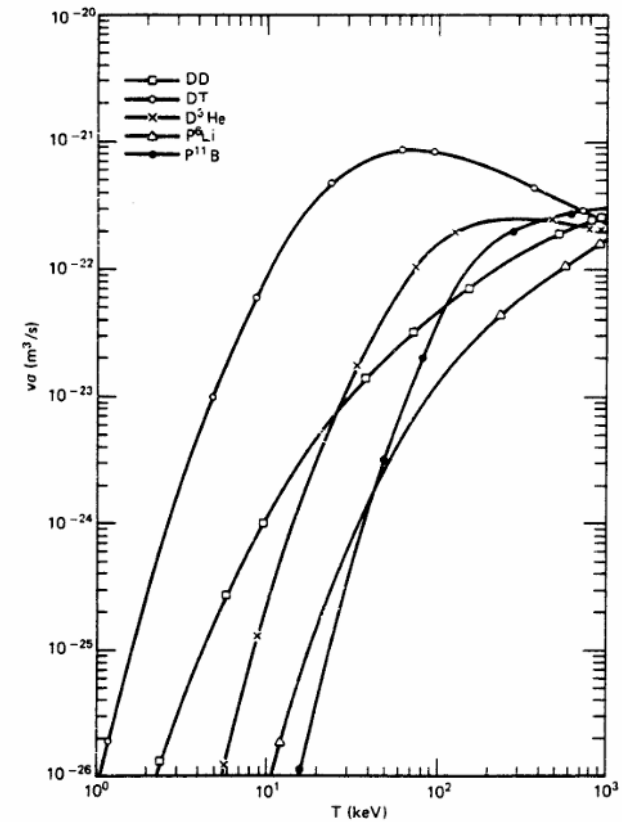


Figure 8.1: Fusion cross section as a function of temperature for a number of isotopes of hydrogen. Note the largest cross section is for the D-T reaction.

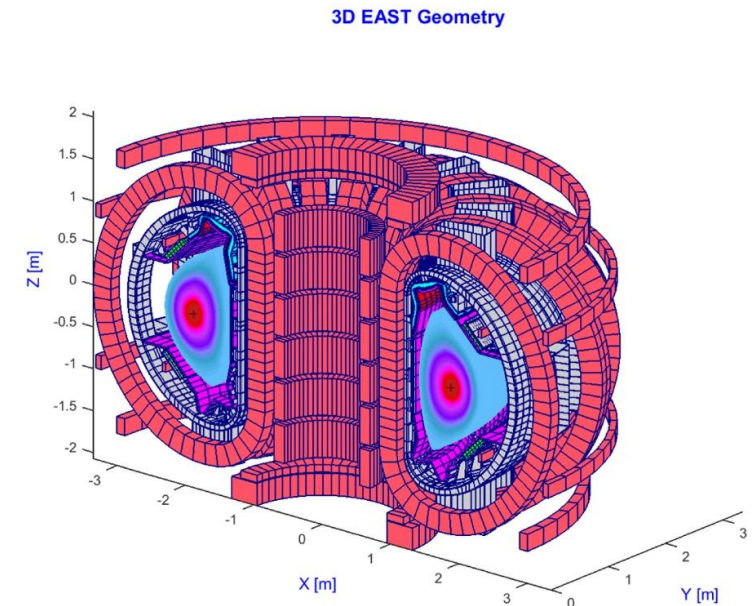
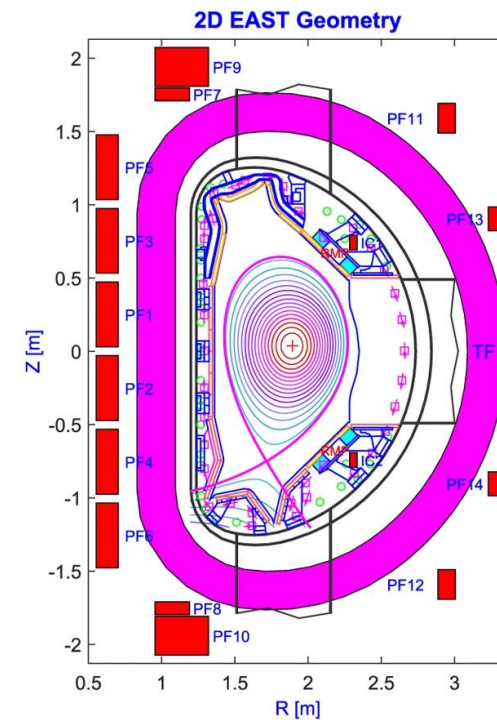
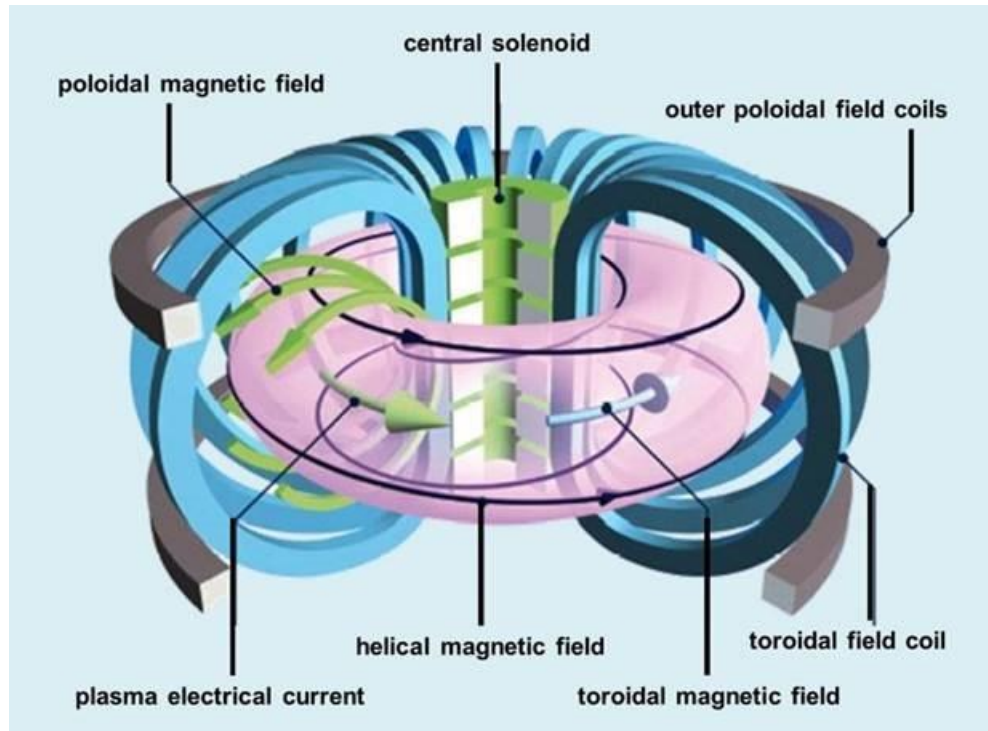
# 一些概念

- Ignition
- $\beta = P_{plasma\ kinetic} / P_{magnetic}$
- $Q_{scientific}$ 与 $Q_{engineering}$

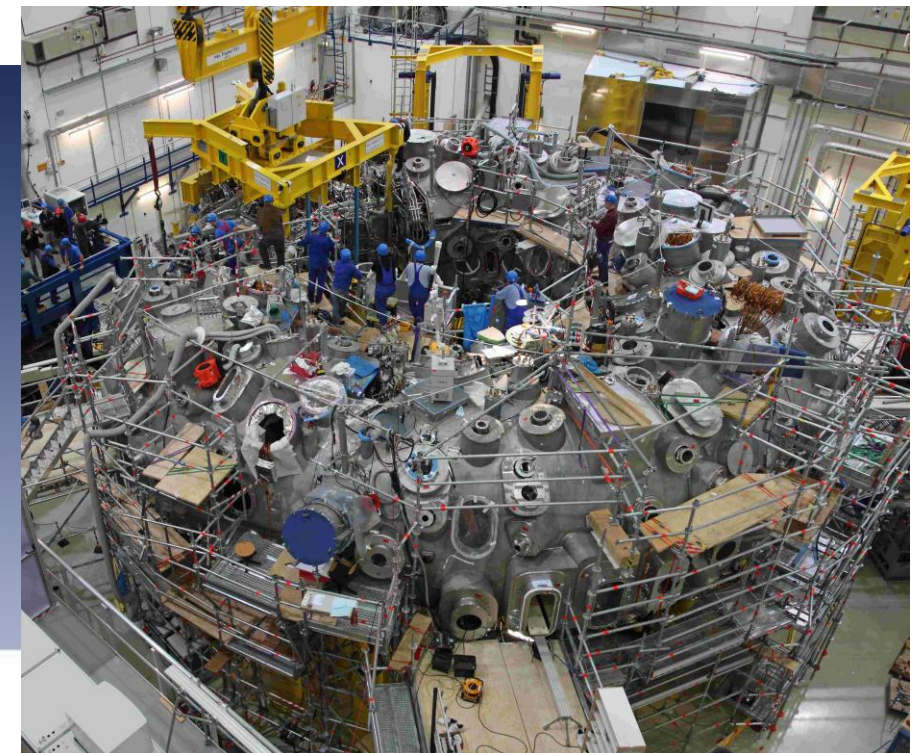
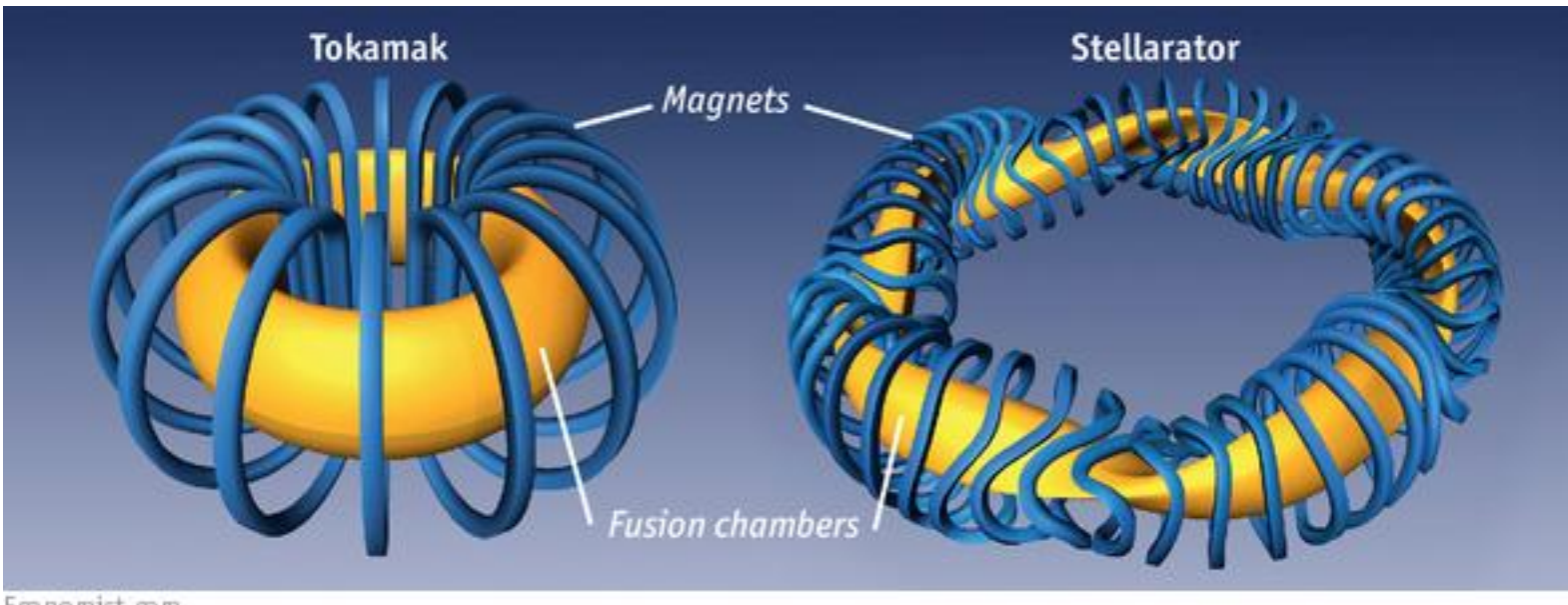
# 诸技术路线

- Magnetic Confinement 磁约束
  - Tokamaks 托卡马克
  - Stellarator 仿星器
  - Z-pinch (?) [ 代表公司 Zap Energy, 为 Uni of Washington 的 spinout ]
  - Magnetic mirror (???)
- 图片在后面三页

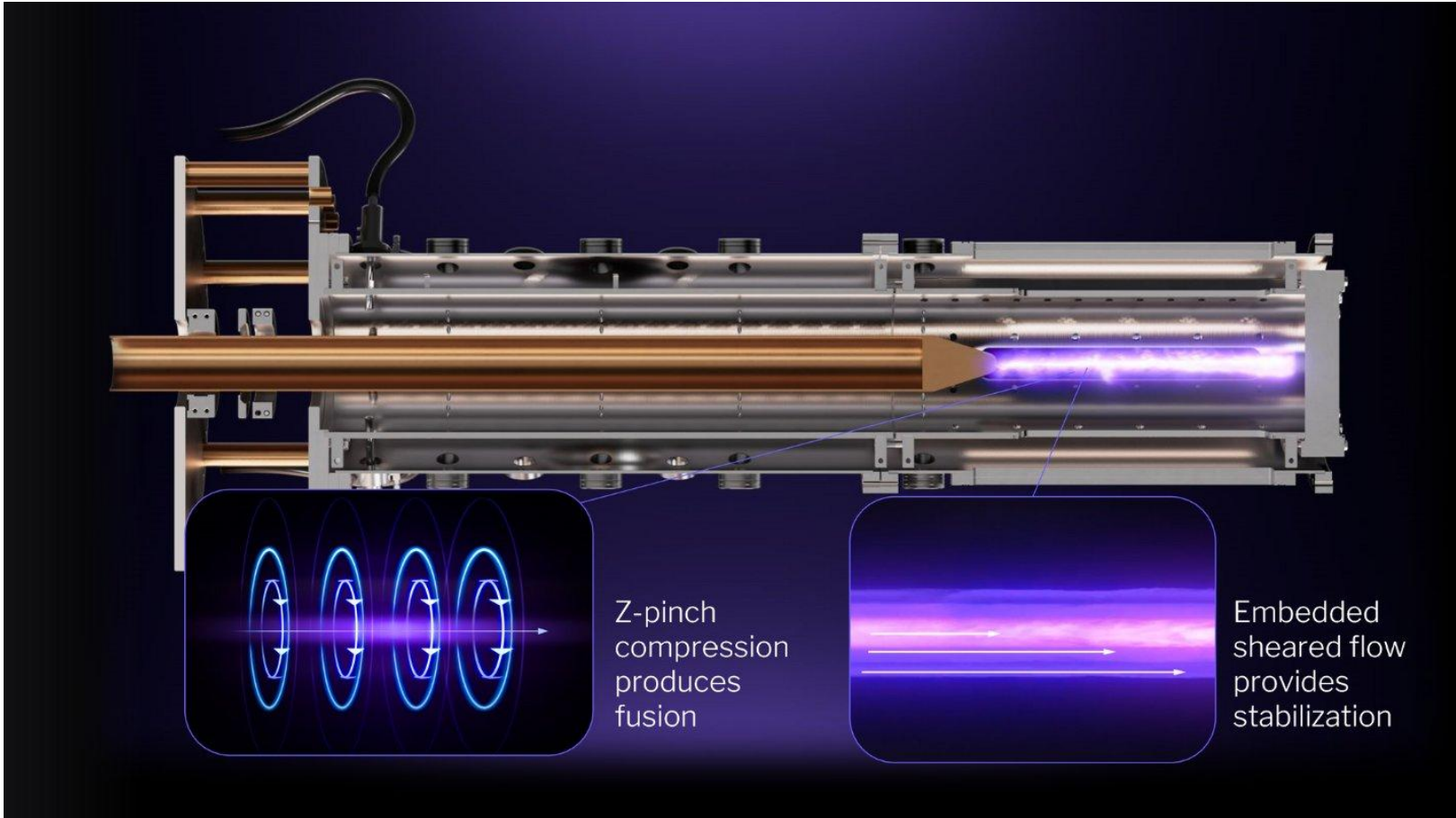
# Tokamaks



# Stellarators



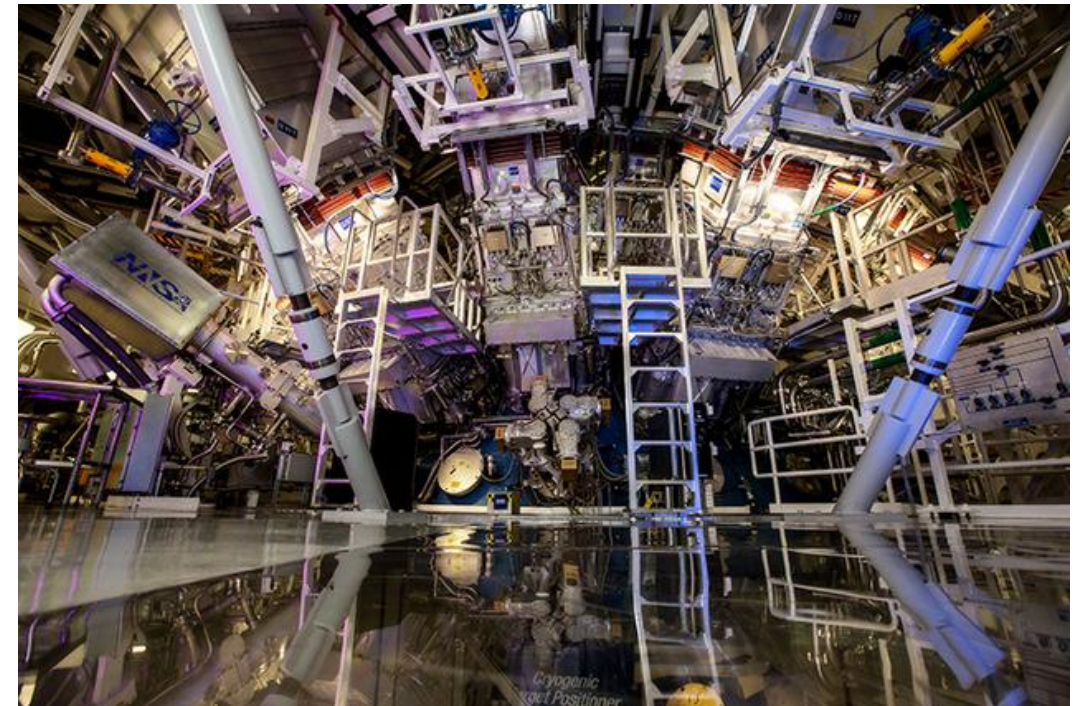
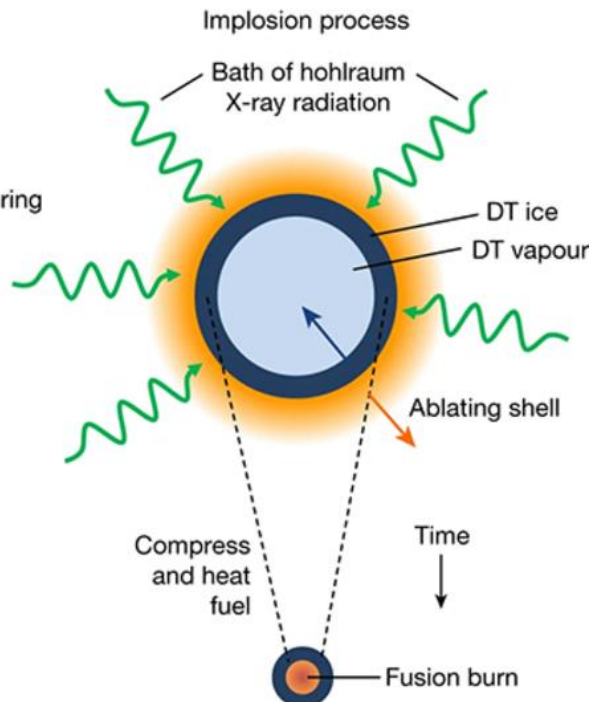
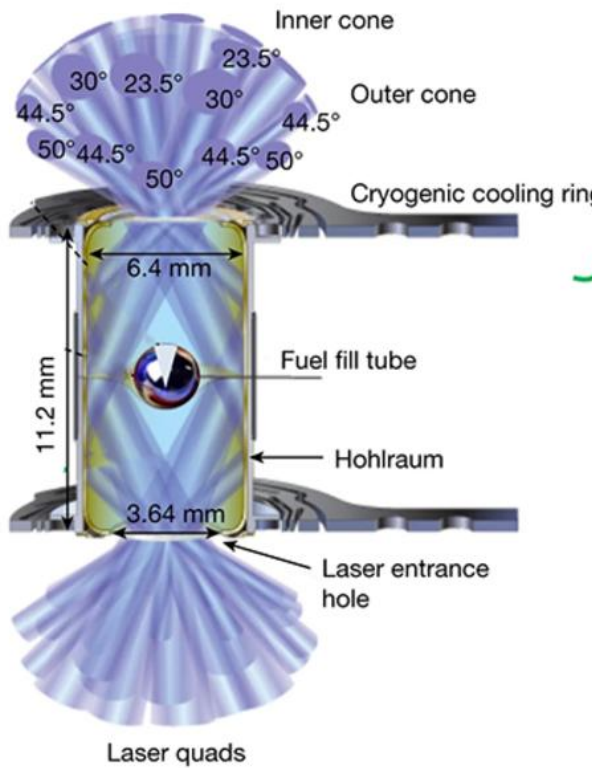
# Z-pinch



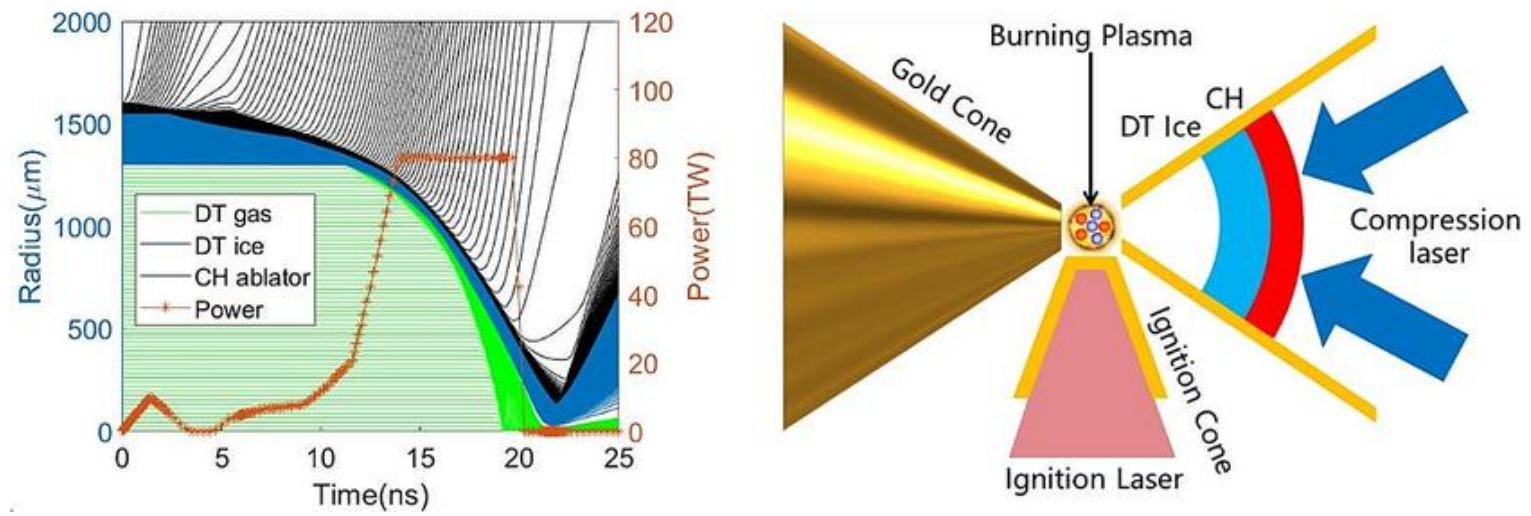
# 诸技术路线

- Inertial Confinement Fusion (ICF) 惯性约束核聚变
  - Laser (Spherically Symmetric: Direct/Indirect; Double-cone Ignition Scheme)
  - Heavy Ion (Direct/Indirect)
  - Liquid Metal (?) [ 代表公司 General Fusion ]
- Magnetic Inertial Confinement (?)
  - [ 代表公司 Helion ]
- 图片在后四页
- And so on

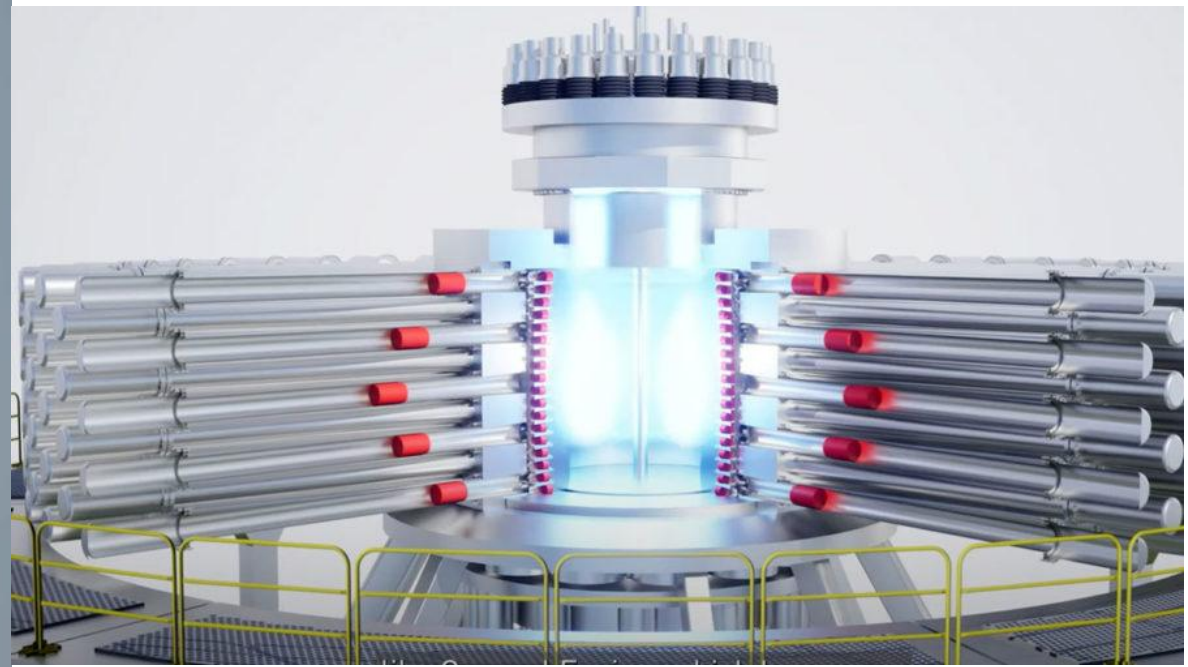
# Laser ICF (Spherically Symmetric; Indirect)



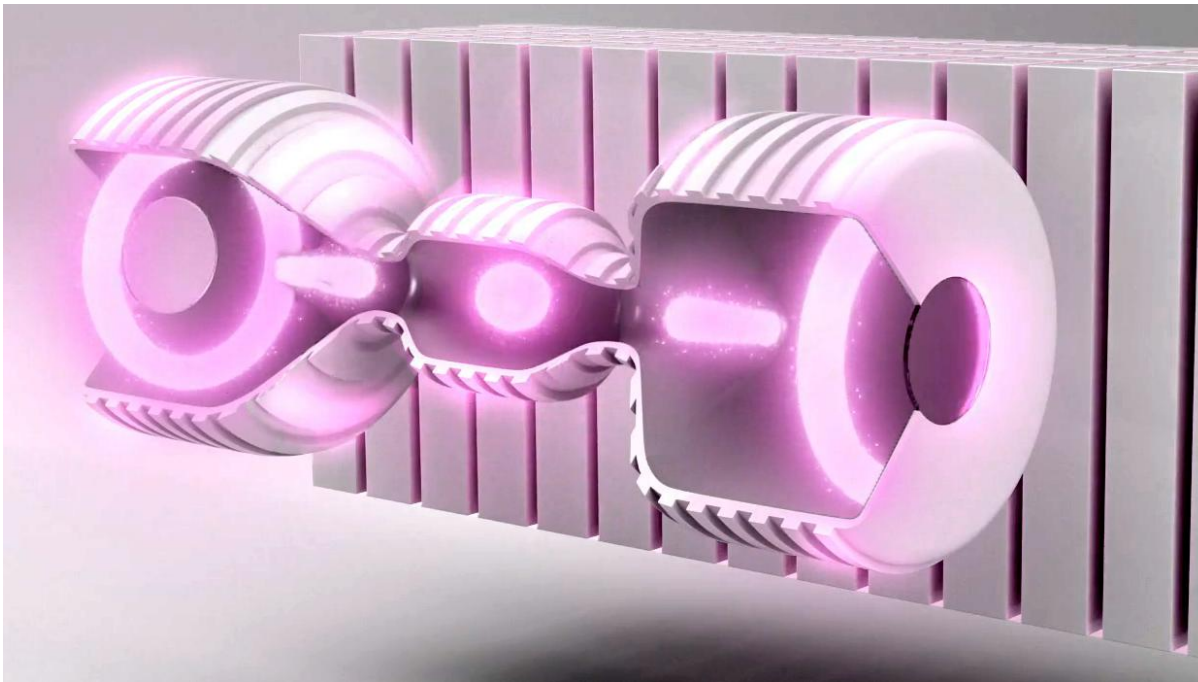
# Laser ICF by Double-cone Ignition Scheme



# ICF by liquid metal [ General Fusion ]



# Magnetic Inertial Confinement [ Helion ]



# 近期进展

- Lawrence Livermore National Lab (LLNL) 的  $Q_{scientific} > 1$  展示
  - Indirect Laser ICF
- REBCO 之于 YBCO 作为超导线材
- 融资热 各国的初创公司

# Intro to Tokamaks

# 参考文献

- Notes on Tokamak equilibrium
- IEEE 系列合集之
  1. Fusion, tokamaks, and plasma control: an introduction and tutorial
  2. Advances in real-time plasma boundary reconstruction: from gaps to snakes
  3. Plasma shape control for the JET tokamak: an optimal output regulation approach
  4. Magnetic control of plasma current, position, and shape in Tokamaks: a survey on modeling and control approaches
  5. Emerging applications in tokamak plasma control
  6. Plasma control in ITER
- 本质上是 literature review , 图文并茂 内有众“Tutorials”可供阅读 不枯燥 易入门
- 前四篇为2005年出版 后两篇为2006年出版 欢迎来到00年代

# 参考文献链接

- Notes on Tokamak equilibrium:
- [https://youjunhu.github.io/research\\_notes/tokamak\\_equilibrium\\_h\\_tlatex/tokamak\\_equilibrium.html](https://youjunhu.github.io/research_notes/tokamak_equilibrium_h_tlatex/tokamak_equilibrium.html)
- IEEE literature review:
  - <https://ieeexplore.ieee.org/document/1512794>
  - <https://ieeexplore.ieee.org/document/1512795>
  - <https://ieeexplore.ieee.org/document/1512796>
  - <https://ieeexplore.ieee.org/document/1512797>
  - <https://ieeexplore.ieee.org/document/1615272>
  - <https://ieeexplore.ieee.org/document/1615274>

# 托卡马克的坐标系

- Axisymmetric!
- $\psi_p$  ( $p=poloidal$  or  $p=plasma$ ) 接下来解释

## Tutorial 1: Flux and Field

A time-varying source of current  $I$  produces a magnetic (vector) field  $B$  that varies directly with the time-varying current. The units of magnetic field commonly used in tokamak plasma physics are the Tesla (T) and the gauss ( $1\text{T} = 10^4 \text{ G}$ ). Magnetic flux is defined as the integral  $\psi = \int_A \mathbf{B} \bullet d\mathbf{A}$  of the field  $B$  through a surface of area  $A$ . Thus, references to flux must implicitly include the area that defines that flux. Units of flux are commonly given in Webers. (See also Table 1.)

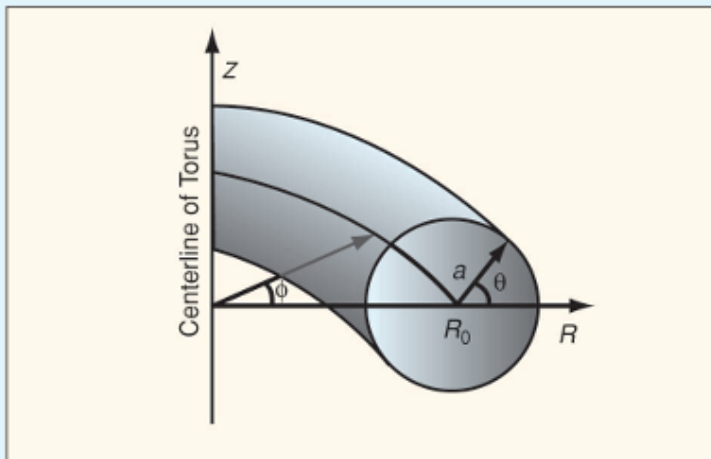


**Figure A.** A plasma having a circular cross section showing standard notation. The cylindrical coordinates are the radial and vertical positions  $R$  and  $Z$ , as well as the toroidal angle  $\phi$ , which measures the angle around the centerline of the torus. The distance to the center of the plasma  $R_0$  is the major radius. The radius  $a$  of the plasma cross section is the minor radius, a terminology used even with noncircular plasmas. The angle  $\theta$  is the poloidal angle. The ratio  $R_0/a$  is the aspect ratio. The midplane of the torus refers to the plane  $z = 0$ .

The analysis of tokamak physics usually considers the toroidal field (or flux) and the poloidal field (flux) separately. The toroidal field is the component of the magnetic field directed in the  $\phi$  coordinate direction of the standard cylindrical coordinates (Figure A). The poloidal field is any field orthogonal to  $\phi$ , that is, in the  $(R, z)$  plane of Figure A.

The models used for tokamak control have frequent need for equations relating current (either in actuating coils or induced in conducting structures) to magnetic flux and field at various locations within the tokamak. Standard magnetics calculations [7] are used to obtain the linear relationships required. The flux  $\psi_S$  through a surface  $S$  is given by  $\psi_S = M_{S1}I_1 + M_{S2}I_2 + M_{S3}I_3 + \dots + M_{Sn}I_n$  using the mutual inductances  $M_{Sk}$  between a finite number  $n$  of conductors carrying currents  $I_k$  and the boundary of the surface  $S$ . Whether the boundary represents a conducting loop or the conductor is imaginary, the calculation is the same.

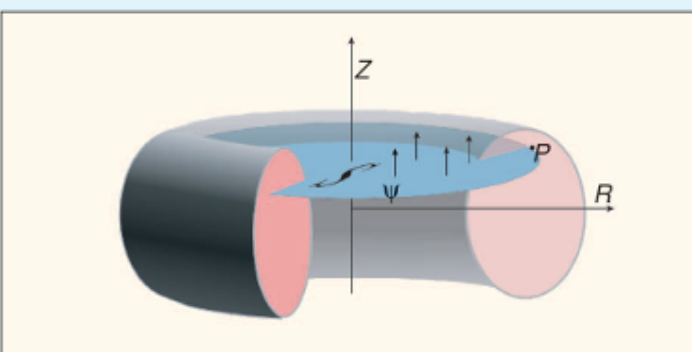


**Figure B.** Definition of the poloidal flux function. The poloidal flux  $\psi_p$  at a point  $P$  in the  $(R, z)$  cross section of the plasma is the total flux through the surface  $S$  bounded by the toroidal ring passing through  $P$ .

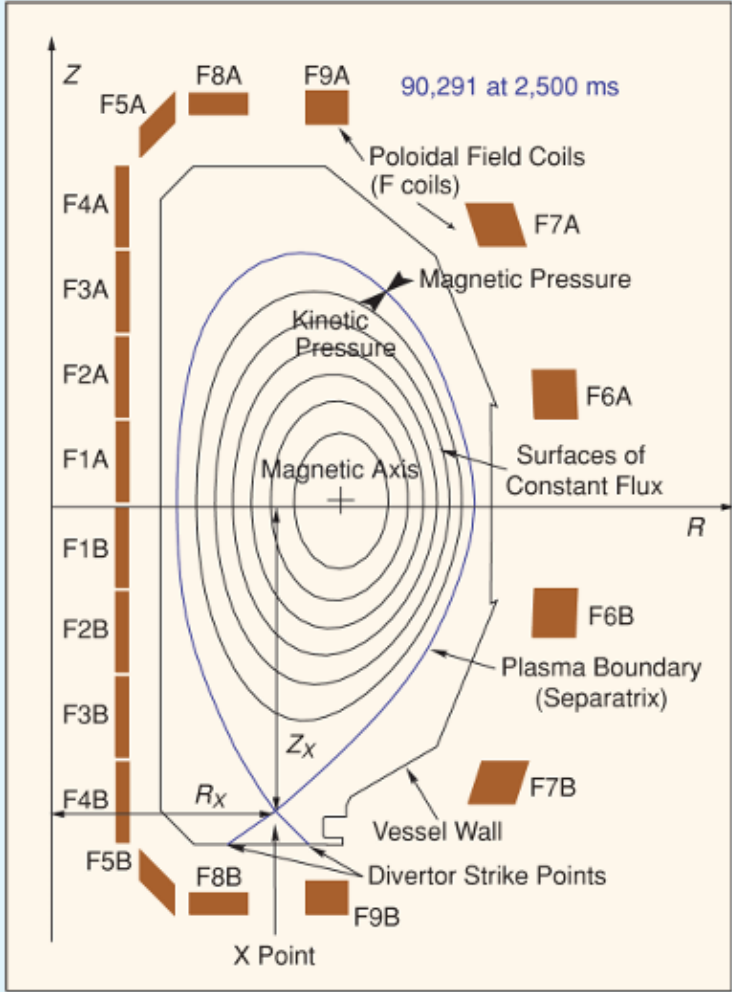


**Figure C.** Cross section of the DIII-D tokamak showing a flux contour representation of the plasma. Note the nesting of contours of constant flux as assumed by ideal MHD (see “Tutorial 3”). The value of flux is largest at the center of these nested flux contours at the magnetic axis. The closed flux surface farthest from the magnetic axis (also called last closed flux surface or separatrix) defines the edge of the plasma. In a diverted plasma, the separatrix forms an X point, in this case at the bottom of the plasma. The points at which the separatrix strikes the vessel wall are strike points. The location of the plasma separatrix and the X point (or strike points) are controlled by the poloidal field generated by currents in the poloidal field coils (whose cross section is labeled F1A through F9B here).

the axis of revolution of the torus (Figure B). The poloidal flux function  $\psi_p = \psi_p(R, z)$  can be defined over the cross section of the vacuum vessel (Figure C). The magnetic field can be obtained through this computation of flux. The integral relation above has an inverse relation

$$B_p = \frac{1}{2\pi R} \left[ -\frac{\partial \psi_p}{\partial z} \quad \frac{\partial \psi_p}{\partial R} \right],$$

which provides the poloidal field at  $P$ , where  $\psi_p$  is the value of poloidal flux at the point  $P = (R_p, z_p)$ .

A terminology commonly used in tokamak control, especially in terms of shape and position, is one of the values of poloidal flux  $\psi_p$  at a point  $p = (R_p, z_p)$ . In this case,  $\psi_p$  is defined as the total flux through a surface bounded by a ring passing through the point  $P$  and concentric with

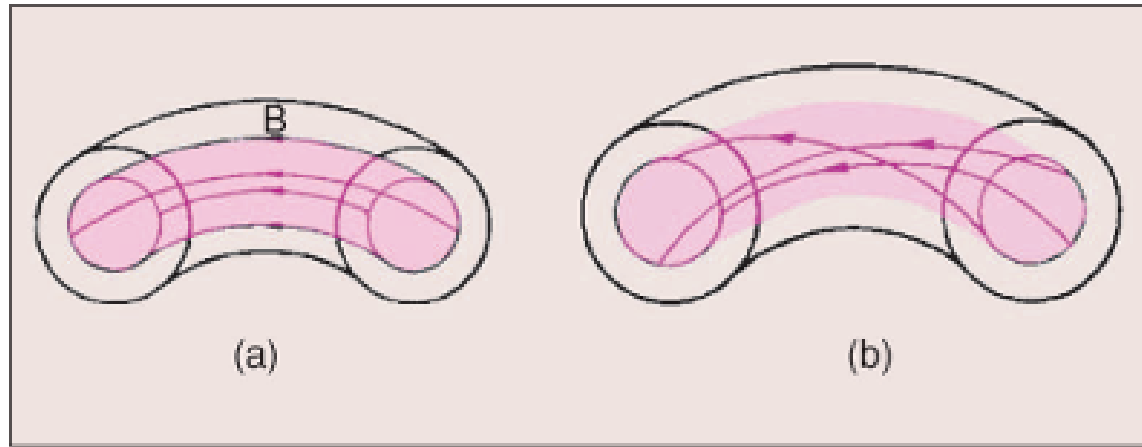


**Figure 9.** *The field lines produced by the toroidal and poloidal field coils (see Figure 4). (a) In a tokamak, the toroidal magnetic field lines are produced by the toroidal field coils (the cream-colored conducting coils in Figure 4). The symbol  $B$  is the standard notation for magnetic field. (b) Addition of a poloidal field by current flowing in the poloidal field coils (light blue coils in Figure 4) and in the plasma produces a combined field in which the magnetic field lines are helical. (Image courtesy of General Atomics Fusion Education Outreach.)*

# 托卡马克的坐标系

- 重要结论：
  - $\psi_p$  的 contour 是磁感线在横截面上的投影！
  - 带电粒子沿磁感线 gyro，所以  $\psi_p$  的 contour 恰恰就是 plasma 的 boundary！
- 在参考文献 Notes on Tokamak equilibrium (P1~P7) 里有关于以上结论的详细推导，感兴趣的诸位可以前往细读

# 托卡马克之 Grad-Shafranov equation

## Tutorial 15: Derivation of the Fundamental PDE and the Grad-Shafranov Equation

The dynamics of the quantities of interest for position and shape control in a tokamak are governed by quasi-stationary Maxwell's equations, given by

$$\nabla \times \mathbf{E} = -\frac{\partial \mathbf{B}}{\partial t}, \quad (1)$$

$$\nabla \times \mathbf{H} = \mathbf{J}, \quad (2)$$

$$\nabla \cdot \mathbf{B} = 0, \quad (3)$$

with the constitutive relationships

$$\mathbf{B} = \mu \mathbf{H}, \quad (4)$$

$$\mathbf{J} = \sigma(\mathbf{E} + \mathbf{v} \times \mathbf{B} + \mathbf{E}_i), \quad (5)$$

where  $\mathbf{E}$  is the electric field,  $\mathbf{B}$  is the magnetic flux density,  $t$  is the time,  $\mathbf{H}$  is the magnetic field,  $\mathbf{J}$  is the current density,  $\mu$  is the magnetic permeability,  $\sigma$  is the electric conductivity,  $\mathbf{v}$  is the velocity, and  $\mathbf{E}_i$  is the impressed field, namely, the force per unit charge due to external sources.

Equation (1), where  $\nabla \times$  is the curl operator, is Faraday's law of electromagnetic induction in its differential form. Equation (2) is Ampère's law, where the term related to the displacement current is neglected; with this assumption, valid for systems where the electric field does not vary too rapidly, the current density is divergence free. Equation (3), where  $\nabla \cdot$  is the divergence operator, is Gauss's law for magnetism. Equations (4) and (5) express the material properties for a class of media that are present in a tokamak. In particular, (5) is Ohm's law in its local form.

In the plasma region, the Lorentz term  $\mathbf{v} \times \mathbf{B}$  has an important effect. The plasma velocity is determined by the momentum balance

$$\rho \left( \frac{\partial \mathbf{v}}{\partial t} + \mathbf{v} \cdot \nabla \mathbf{v} \right) = \mathbf{J} \times \mathbf{B} - \nabla p, \quad (6)$$

where  $\nabla$  is the gradient operator and  $p$  is the kinetic pressure. Pressure, velocity, and density are coupled by thermodynamic and fluid equations. For a single, nondissipative fluid involving adiabatic behavior and entropy conservation, the thermodynamic equation has the form

$$\frac{\partial(p\rho^{-\gamma})}{\partial t} + \mathbf{v} \cdot \nabla(p\rho^{-\gamma}) = 0, \quad (7)$$

where  $\rho$  is the mass density and  $\gamma$  is the gas adiabatic exponent. Finally, mass conservation yields the continuity equation

$$\frac{\partial \rho}{\partial t} + \nabla \cdot (\rho \mathbf{v}) = 0. \quad (8)$$

In axisymmetric geometry with cylindrical coordinates  $(r, \phi, z)$ , the vectors  $\mathbf{B}$  and  $\mathbf{J}$  can be expressed in terms of two scalar functions, namely, the poloidal magnetic flux and the poloidal current. The poloidal flux  $\Psi(r, z)$  is the magnetic flux linked with the circumference obtained by revolving the point  $(r, z)$  around the  $z$  axis. The vertical component of  $\mathbf{B}$  is then given by  $B_z = (\partial \Psi / \partial r) / 2\pi r$ , as can

be verified by considering the differential magnetic flux  $d\Psi = \Psi(r + dr, z) - \Psi(r, z)$ . Rather than the poloidal flux, the poloidal flux per radian  $\psi(r, z) = \Psi(r, z) / 2\pi$  is more frequently used to simplify the expressions, yielding  $B_z = (\partial \psi / \partial r) / r$ . In addition, the divergence-free condition (3) yields the radial component  $B_r = -(\partial \psi / \partial z) / r$ , since the differential flux  $d\Psi = \Psi(r, z + dz) - \Psi(r, z)$  is exactly balanced by the magnetic flux across the lateral cylindrical surface, where  $B_r$  is the normal component and  $dz$  is the height.

Using Ampère's law (2) and the constitutive equation (4), the total current linked with the circumference obtained by revolving  $(r, z)$  around the  $z$  axis is given by  $I_{\text{pol}}(r, z) = 2\pi r B_\phi(r, z) / \mu(r, z)$ . The poloidal current function  $f = \mu I_{\text{pol}} / 2\pi = r B_\phi$  is introduced to remove the coefficient  $2\pi/\mu$ . Therefore, the magnetic flux density can be expressed as

$$\mathbf{B} = \frac{1}{r} \nabla \psi \times \mathbf{i}_\phi + \frac{f}{r} \mathbf{i}_\phi, \quad (9)$$

where  $\mathbf{i}_\phi$  is the unit vector in the toroidal direction (see "Tutorial 1" in [1]).

A similar expression can be derived for the current density

$$\mathbf{J} = \frac{1}{r} \nabla \left( \frac{f}{\mu} \right) \times \mathbf{i}_\phi - \frac{1}{\mu_0 r} \Delta^* \psi \mathbf{i}_\phi, \quad (10)$$

where  $\mu_0$  is the magnetic permeability of the vacuum, the poloidal components  $J_r = -(\partial I_{\text{pol}} / \partial z) / 2\pi r$  and  $J_z =$

$(\partial I_{\text{pol}} / \partial r) / 2\pi r$  are expressed in terms of  $f$ , whereas the toroidal component is related to the second-order differential operator  $\Delta^*$  defined by

$$\Delta^* \psi \equiv r \frac{\partial}{\partial r} \left( \frac{1}{\mu_r r} \frac{\partial \psi}{\partial r} \right) + \frac{\partial}{\partial z} \left( \frac{1}{\mu_r} \frac{\partial \psi}{\partial z} \right), \quad (11)$$

where  $\mu_r = \mu / \mu_0$  is the relative magnetic permeability, which is unity in a vacuum and in nonmagnetic media such as air and plasma. Equation (11) is obtained from the toroidal component of Ampère's law (2) using the constitutive equation (4) and the magnetic flux expression (9) in terms of  $\psi$ .

At equilibrium, the plasma momentum balance (6) becomes  $\mathbf{J} \times \mathbf{B} = \nabla p$ , from which  $\mathbf{J} \cdot \nabla p = 0$  and  $\mathbf{B} \cdot \nabla p = 0$ . In axisymmetric plasmas, taking into account expressions (9)–(10) and that  $\mu = \mu_0$ , these relationships yield  $\nabla p \times \nabla \psi = \nabla p \times \nabla f = 0$ . Hence  $\nabla f \times \nabla \psi = 0$ , and the equilibrium condition  $\mathbf{J} \times \mathbf{B} = \nabla p$  becomes

$$-\mu_0 \frac{\Delta^* \psi}{r^2} \nabla \psi - \frac{f}{\mu_0 r^2} \nabla f = \nabla p, \quad (12)$$

giving the Grad-Shafranov equation

$$\Delta^* \psi = -f \frac{df}{d\psi} - \mu_0 r^2 \frac{dp}{d\psi}, \quad (13)$$

where  $\Delta^*$  is defined by (11).

# 托卡马克之 Grad-Shafranov equation

giving the Grad-Shafranov equation

$$\Delta^* \psi = -f \frac{df}{d\psi} - \mu_0 r^2 \frac{dp}{d\psi}, \quad (13)$$

where  $\Delta^*$  is defined by (11).

$$\Delta^* \psi \equiv r \frac{\partial}{\partial r} \left( \frac{1}{\mu_r r} \frac{\partial \psi}{\partial r} \right) + \frac{\partial}{\partial z} \left( \frac{1}{\mu_r} \frac{\partial \psi}{\partial z} \right), \quad (11)$$

# 托卡马克在计算机中的建模

- Discretization
- Mutual Inductance matrices
- Circuit Model

$$d\Psi/dt + \mathbf{R}\mathbf{I} = \mathbf{U},$$

where  $\Psi$  is the vector of magnetic fluxes linked with the circuits,  $\mathbf{R}$  is the resistance matrix, and  $\mathbf{U}$  is the vector of applied voltages. The magnetic fluxes linked with the circuits depend on the magnetic configuration and therefore are functions of  $\mathbf{I}$ ,  $\beta_{\text{pol}}$ , and  $\ell_i$  (further details are given in "Derivation of Circuit Equations.")

$$d(\mathbf{LI})/dt + \mathbf{RI} = \mathbf{U}, \quad (7)$$

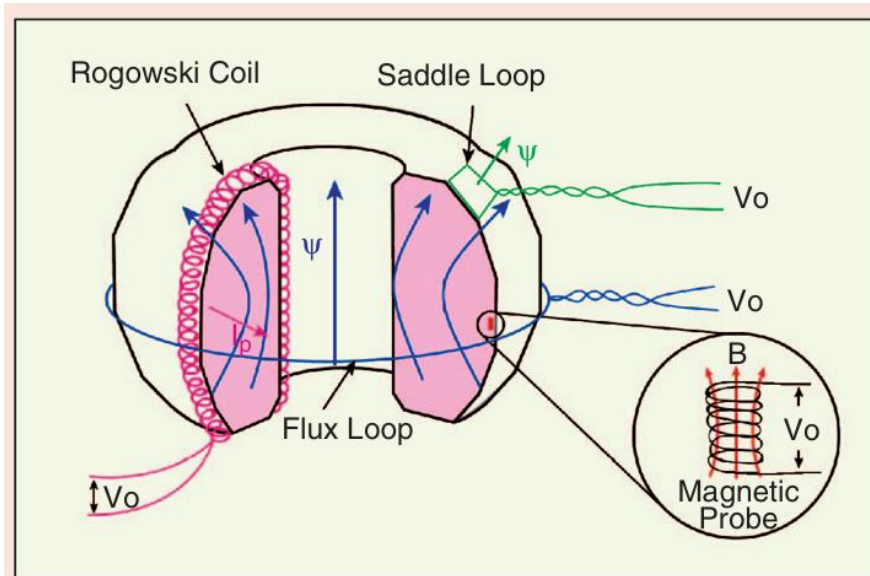
where  $\mathbf{U}$  is the vector of voltages applied to the circuits (nonzero for the active coils),  $\mathbf{R}$  is the circuit resistance matrix, and  $\mathbf{L}$  is the matrix of self- and mutual inductances between the plasma, the coils, and the equivalent circuits of the passive structures [30], [31]. It should be noted that

# 托卡马克在计算机中的建模

- 具体求解这个系统的时候，通常需要把 circuit model , Grad-Shafranov equation , 还有一些其他七七八八的东西给耦合起来 . 过程比较复杂 这里暂且不表 .

# 托卡马克之边界重构 (Boundary Reconstruction)

- 测量 by coils & loops
- 测量 by a bunch of other things



*Magnetic diagnostics. All of these sensors operate on the same basic principle, namely, changing flux induces a voltage in a coil of wire. This voltage is integrated to determine the flux through the coil.*

# 托卡马克之边界重构 (Boundary Reconstruction)

- EFIT (Equilibrium FITting , 业界常用软件) : 将测量结果 fit 进 Grad-Shafranov equation 中 然后求得我们想要的一些关于当前 equilibrium 的信息
  - 我目前理解应该有两种大致上的模式分类 : 一种是实时 equilibrium reconstruction 然后必须使用一些简化版本的 GS equation 比如说 locally linearized , 从而提升计算速度 ; 另一种是事后复盘所以有充足的时间 所以会用完整的 GS equation 来大炫特炫

# 托卡马克之边界重构 (Boundary Reconstruction)

- 描述方式: Flux v.s. Gap
- 但是其实现在不存在绝对的非此即彼

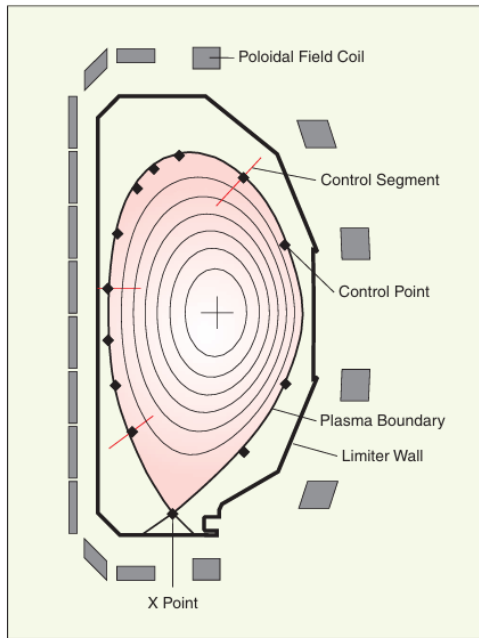


**Figure 5.** Layout of the DIII-D tokamak. The poloidal cross section of this tokamak highlights the position of the shaping field coils and the points for the isoflux control system (diamonds). The drawing represents a single null divertor discharge.

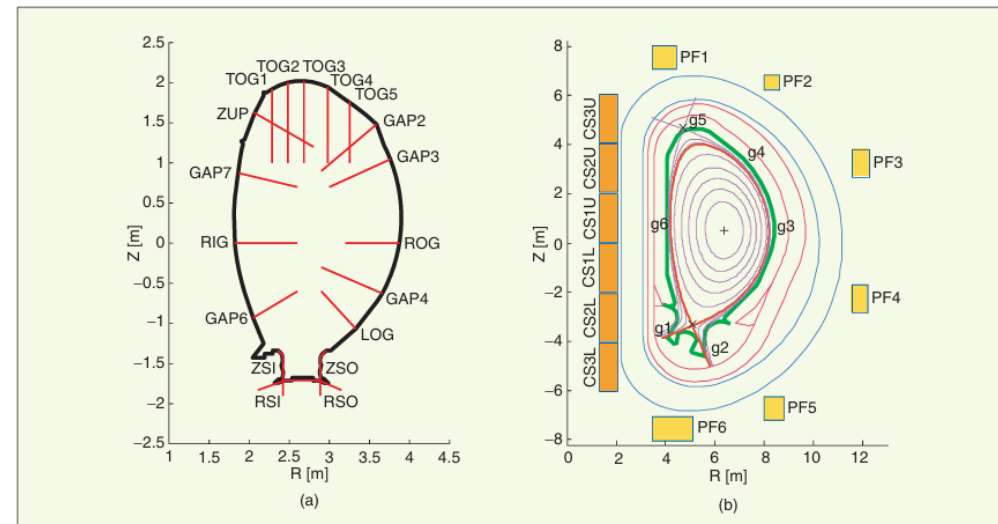


**Figure 6.** Gap location for (a) JET and (b) ITER. The gap location is chosen semiempirically at JET according to experimental needs, while for ITER an optimal placement procedure is adopted. In any case, the gap approach suffers from the local nature and arbitrariness in the definition of the gaps.

# 托卡马克之边界重构 (Boundary Reconstruction)

- 古早计算机视觉之 “Snakes”
- 当代计算机视觉之 Neural Networks

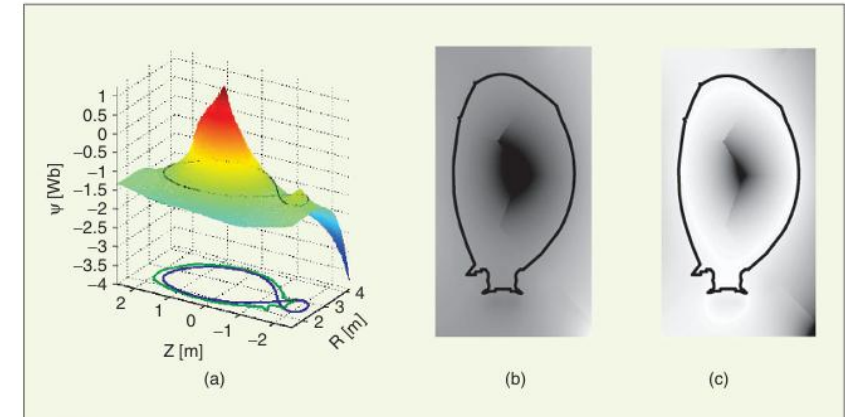
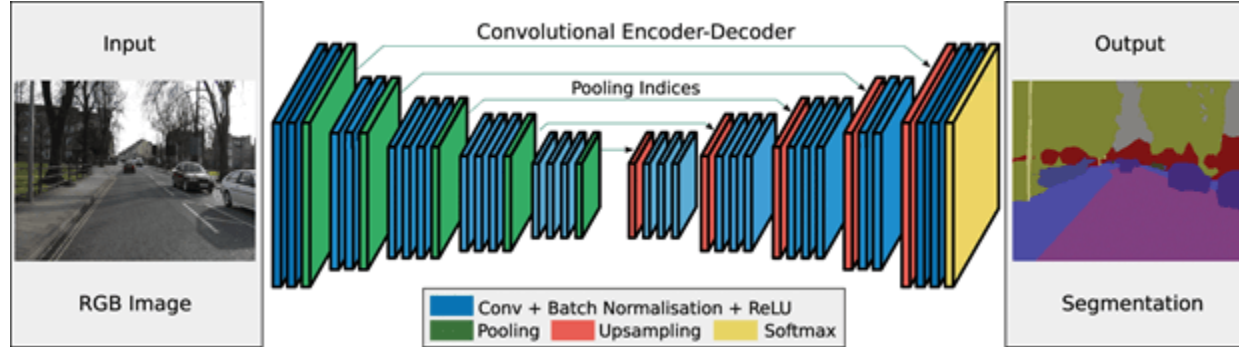


**Figure 8.** The plasma image whose edge is to be detected. (a) The intensity of the flux map as defined by the XLOC algorithm is shown as a 3-D function to better appreciate the energy landscaping idea and the curve-sliding procedure. The first-wall and plasma boundary are superimposed to elucidate the meaning of the flux map. (b) The 2-D initial flux map is modified by subtracting the flux at (c) the boundary, defined as the maximum of the flux at the X point and over the plasma-facing surfaces. The resulting boundary image suggests the use of active vision techniques for edge detection.

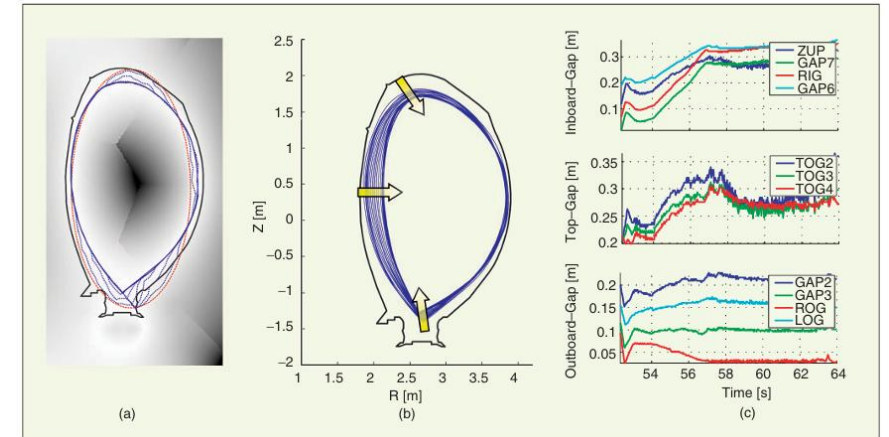


**Figure 11.** Tracking a plasma shape with the active contour technique for JET pulse #57989. (a) Convergence to the initial shape. The dashed red line is the initial contour, the dotted curves are the iterations, and the blue solid line is the detected boundary. The curves shown for successive iterations follow the flux map grid points, and thus appear to be less smooth than the final contour. (b) The evolution during the discharge. The deformation of the plasma shape is evident. The configuration changes from a standard shape to a highly triangular one, with deformations mainly in the inner part of the boundary and the position of the X point. (c) The gap behavior is plotted as a function of time. The gaps, which are located as shown in Figure 6, are grouped according to the position on the poloidal cross section. From these waveforms the actual deformation of the shape is scarcely perceptible.

# 托卡马克之位形控制 (Shape and Position Control)

- 经典方法: linearized model + feedback loop with PID controllers
  - 对 linearization 的需求如之前的解释那样 是为了给计算提速；至于具体这个被 linearized 的 model 长啥样，请移步 IEEE 合集之3
  - PID = Proportional-Integral-Derivative
- 当代尝试: Neural Networks

# 托卡马克之 Instabilities

- 枚举
  - Vertical Instabilities
    - 最后等离子体会撞墙上
  - Neoclassical Tearing Modes (NTM): magnetic islands
    - 会导致等离子体撕裂
  - Edge Localized Modes (ELM): edge-localized energy events in “H-mode”
    - 有能量从barrier里面burst出来了 这你受得了吗
  - Resistive Wall Modes (RWM): plasma kink instability
    - 会导致等离子体能量在短时间内大量流失 从而影响confinement也损坏容器
- 图片见后两页

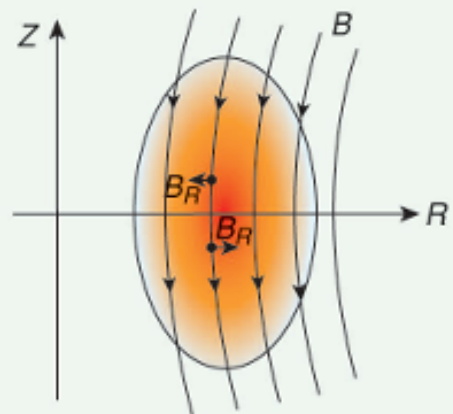


**Figure C.** Illustration of the source of vertical instability. The magnetic field with radial component directed inward above the midplane and directed outward below the midplane is generated by the shaping coils to cause the plasma to become elongated. The  $J \times B$  force for inward (outward) directed magnetic field and positive toroidal current (into the page) is up (down). As long as the current distribution and magnetic field are completely symmetric about the midplane ( $z = 0$ ), the upward and downward forces balance, and the plasma is in equilibrium. If a disturbance shifts the plasma up slightly, more current will be above the midplane than below and the net force is directed upward. This imbalance causes the plasma to move up, thereby further increasing the upward force. A similar situation occurs if the disturbance causes an initial downward displacement of the plasma. This behavior is the essence of the vertical instability.

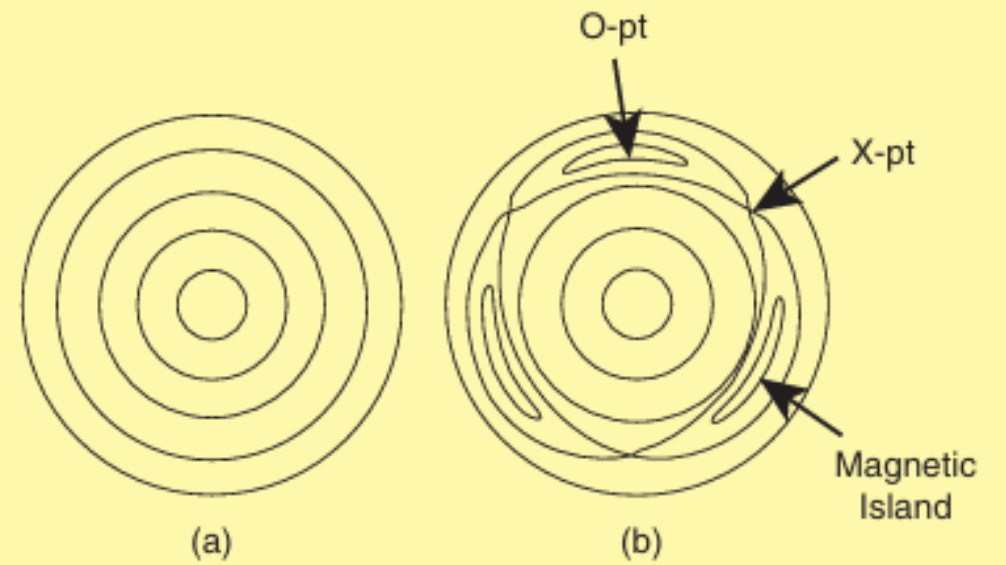


**FIGURE 1** Magnetic island topology in a circular cross-section plasma. (a) Perfectly conducting ideal MHD plasmas (Tutorial 3 in [1]) require nested flux surfaces, (b) while resistive plasmas can produce tearing and reconnection (hence the name *tearing mode*) of flux surfaces, resulting in magnetic islands. The current and pressure profiles (Tutorial 5 in [1]) are flattened across an island, whose center is the *O-point*. The resulting connection between inner and outer island surfaces, joined at the *X-point*, allows heat to leak out of the plasma core faster than it would without the island, thus degrading confinement. (b) shows the island topology corresponding to a 3/2 NTM, which has a periodicity of  $m = 3$  (Tutorial 4 in [1]) in the poloidal cross section shown and a periodicity of  $n = 2$  in the toroidal direction (not illustrated).

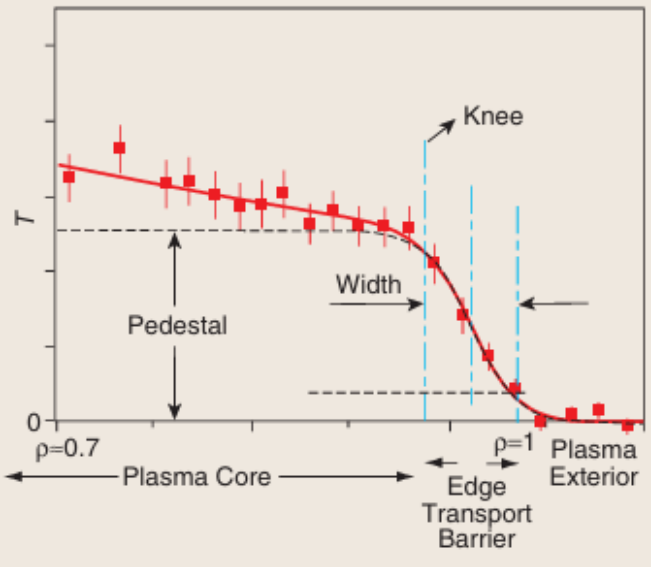


**FIGURE A** Definitions relevant to ELMs. The solid red curve is fit to the measured electron temperature data. Lines through the data points indicate plus or minus one standard deviation (estimated) from measurements. The edge transport barrier (ETB) is a region at the edge of the plasma that is a barrier to the transport, or diffusion, of heat and particles out of the plasma. The ETB and other forms of transport barrier are characteristic of high energy confinement mode (H-mode) plasmas, since they tend to prevent heat from escaping the plasma. Width of the ETB is defined to be the width of the steep gradient region in the electron temperature profile. This edge region is defined to be the region between the knee of the fitting function and the plasma last closed flux surface. The pedestal in temperature coincides with the plasma interior region. (The terminology in the literature is inconsistent, since “pedestal” is sometimes used to refer to the edge region.) Since the pressure profile in H-mode plasmas takes a similar form, in discussions of edge transport barriers, temperature and pressure are often used interchangeably. However, pressure can sometimes have a narrower steep gradient region. The close proximity of the high-pressure region inside the ETB and the low-pressure region outside the ETB is the source of the ELM instability.

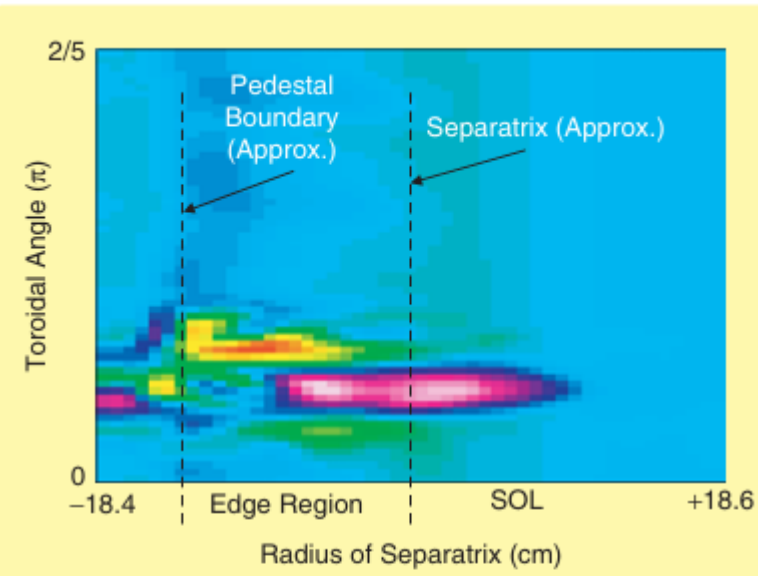


**FIGURE 8** Intensity plot of the perturbed density at the plasma outer midplane during the later nonlinear phase of a simulation of the growth of the edge localized mode. The early phase of the mode growth is linear and approximately represented by ideal MHD. The local nature of the mode growth is illustrated with the “finger” of plasma radiating out from the plasma edge toward the vacuum vessel wall. This plasma finger also extends along the magnetic field (into and out of the page). Large transport through the walls of the finger or the breaking off, or magnetic reconnection, of the finger are possible mechanisms for the ELM energy loss.

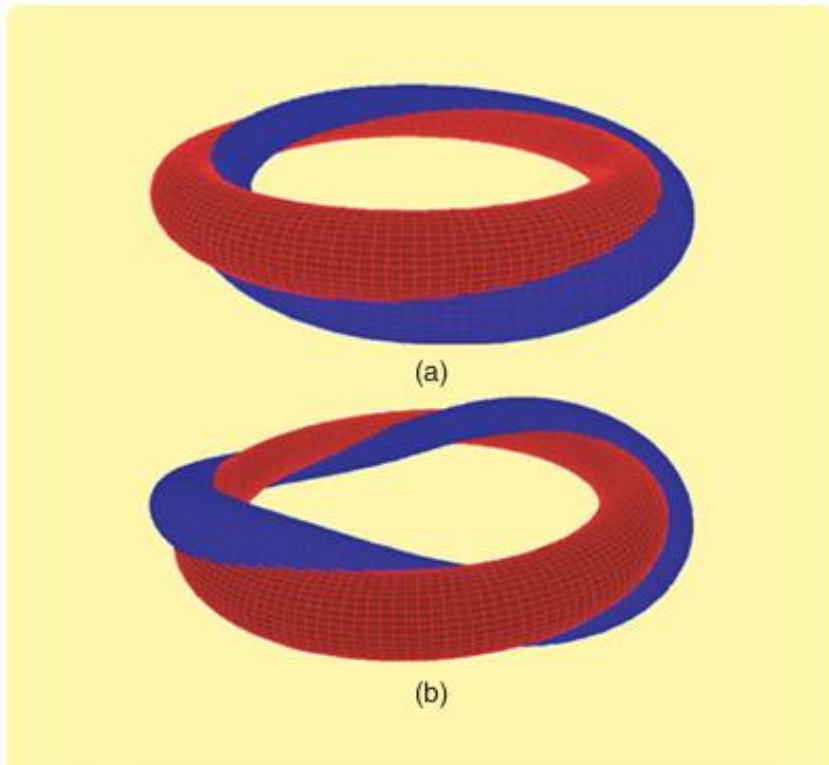


**FIGURE 10** Illustration of kink deformations of a circular cross-section plasma, greatly exaggerated for illustration. The red torus represents a circular cross-section plasma before deformation. The blue surface represents the deformed plasma: (a) shows an  $n = 1$  kink, and (b) shows an  $n = 2$  kink, in which the plasma perturbation repeats itself twice as the toroidal angle varies from 0 to  $2\pi$ . In each case, the deformation follows a helical path with respect to the undeformed plasma.

# 托卡马克之 Instabilities

- 以上的所有 Instabilities 均有解法，详情见 IEEE 系列合集之5
  - “解法”指的是 [ 测量 – 发现 – 控制 – 解决 ]，而非从一开始就杜绝
  - 问题只在于 Instabilities 的强度 v.s. 解法的作用强度
- 梯度与大装置与强(磁)场
  - (e.g. 温度或能量或什么的)梯度越大 越不稳定
  - 大装置空间尺度更大 所以同等能量下梯度更小
  - 更强的磁场意味着更好的约束

# 大家还有什么问题吗

- 首先这是一个大体上的介绍 时间有限 无论是关于fusion本身还是关于tokamaks 都有很多没有触及到的点 . 以后在更漫长的论文交流讨论时期 如果有遇到什么其他的今天没有来得及解释的概念 我会当场解释的 . ~~反正今天全部解释完了你们也不记得~~.
- 我本身也只是刚入门 所以关于你们的问题我大概会有如下三种解答方式：
  - 请移步参考文献中的 e.g. IEEE 系列合集 ( 虽然我不一定记得是哪一份 )
  - 等我读个博回来告诉你
  - \*因为是比较general的问题所以开始大放厥词侃侃而谈\*
- But anyways, I welcome any kind of questions, and feel free to ask.